Int. J. Heat Mass Transfer. Vol. 35, No. 7, pp. 1667–1672, 1992
Printed in Great Britain

0017–9310/92 $5.00 + 0.00

Modification of the wide-band gas radiation model for flame calculation

WŁADYSŁAW KOMORNICKI and JERZY TOMECZEK
Department of Fuel Energy, Silesian Technical University, Katowice, Krasińskiego 8, Poland

(*Received* 9 *May* 1991 *and in final form* 24 *June* 1991)

Abstract—The aim of this paper is to present a modification of the wide-band gas radiation model suitable for a non-homogeneous layer. The application of this modification has been compared with the literature models of radiation in standard conditions and in large diffusion flames. It has been shown that the proposed modification allows an increase of accuracy of radiation intensity calculation by the wide-band model. Experimental verification of calculated radiation intensity for a 750 kW natural gas flame is presented.

1. INTRODUCTION

LARGE gradients of temperature, chemical composition and soot concentration within flames cause non-homogeneity of flame radiation properties. Measurements have shown that flames form strongly non-gray bodies [1]. Consequently, radiation heat transfer within the flames can be accurately predicted only by application of the narrow-band model [2]; however, it requires a long computational time. The wide-band model is much faster [3, 4], but its suitability for a non-homogeneous layer is limited. Non-spectral models [5–8] are very efficient in calculations but their accuracy is poor in a non-homogeneous layer.

Application of the narrow-band radiation model to comprehensive calculation of large flames requires long computational times, while the faster wide-band Edwards model and the even faster non-spectral models can deform the radiation intensity profiles to an extent contrasting with the experimental profiles. A new method of calculation of the absorptivity of the wide-band model is proposed in this paper, which allows the prediction of radiation heat transfer within a non-homogeneous layer with the accuracy of the narrow-band model. Absorptivities of the bands were calculated based on the narrow-band model and are tabulated as functions of the temperature and optical depth. The modified wide-band model has been verified on the bases of non-homogeneous temperature and concentration profiles [6] and was successfully applied to radiation intensity calculation within an industrial natural gas luminous diffusion flame. Very good convergence of the experimental and calculated radiation intensity distributions has been obtained by means of the measured values of soot concentration, temperature and gas composition.

2. RADIATION MODEL

Within a luminous flame both the gases and soot contribute to the radiation flux of the flame. The radiation properties of soot are relatively well described in the literature in a form suitable for non-homogeneous layer calculation [9]. There are, however, problems with the determination of radiation properties of gases applicable to non-gray flame modelling. The non-spectral models have very short computation times but on the other hand they are limited in applications. The model proposed by Hottel and Sarofim [5] of the sum of gray gases has elaborated coefficients only for cases in which the ratio of water vapour to carbon dioxide is constant: 2 for gaseous flames [10] and 1 for oil flames [11]. That developed by Grosshandler, the Total Transmittance Non-Homogeneous model (TTNH) [6], is based on a faulty integral form of the solution of the radiation equation (equation (1) in ref. [6]). This faulty form appears to be the reason for some wrong interpretation in the literature [6, 12, 13]; thus, it is worth presenting here the correct form of this equation which for a cold background can be written as

$$i = \exp\left(-\int_0^L k_\omega \, \mathrm{d}l\right) \int_0^L i_b \exp\left(\int_0^l k_\omega \, \mathrm{d}l^*\right) k_\omega \, \mathrm{d}l. \tag{1}$$

Another form of this equation is presented by Siegel and Howell [14].

The narrow-band model allows the calculation of gas radiation properties for each spectral line. In this model the linear absorptivity spectral coefficient depends on two parameters: the mean spectral line intensity and the spectral line width. These parameters were measured and tabulated as a function of wave number and temperature for water vapour, carbon dioxide and carbon monoxide [15]. Fragmentation of the whole spectrum into narrow bands of 2500 m^{-1} wave number width requires scanning over 350 narrow-band regions.

The wide-band model reduces this number to 12 bands. In this model two parameters have to be determined for each band: the optical depth at the band

NOMENCLATURE

a	band absorptivity	L	total path length [m]
A	band absorption [m^{-1}]	n	refractive index
c	soot concentration [kg m^{-3}]	p	pressure [Pa]
i	spectral radiation intensity [W m^{-1} sr^{-1}]	T	temperature [K].
i_b	spectral black body radiation intensity [W m^{-1} sr^{-1}]		
k	absorption index	Greek symbols	
k_ω	spectral absorption coefficient [m^{-1}]	ρ	soot density [kg m^{-3}]
l	path length [m]	τ_H	optical depth at band head.

head and the line width parameter. Based on these parameters the absorption, A, of a band can be found and consequently its absorptivity, a, may be calculated from Edwards' [4] equation:

$$a = 1-(\tau_H/A)(dA/d\tau_H). \quad (2)$$

According to Edwards' proposal the absorptivity calculated from equation (2) should not be smaller than 0.1. This method often gives values of band absorptivity different from the equivalent band absorptivity calculated by means of the narrow-band model, in spite of the accurate value of the band absorption A.

A comparison of the 2700 nm band of water vapour calculated by means of the narrow-band model and by means of the wide-band model according to Edwards is presented in Fig. 1. It is clear that the values of absorptivity by both these methods differ significantly. This figure also presents the characteristics of the band according to the present modification, which reflects much better the physical sense of the band. The modified absorptivity of the wide-band model was obtained based on the narrow-band model data, with the assumption that the boundaries of the band can be placed at points where the absorptivity is equal to 5% of the maximum absorptivity within the band. In some cases the boundaries of the bands are not abrupt. Then the boundaries of the modified wide-band are placed at points where the absorptivity is twice as great as the minimum absorptivity of the band end. Dividing the band absorption A, taken from Edwards' model [4], by the so-determined width of the band, we get the modified absorptivity of the wide-band. It can be seen that the centre of the modified wide-band is not placed at a point determining the middle of the band but at a point proposed by the original Edwards model. To enable the application of the modified wide-band model to a non-homogeneous layer the absorptivities of water vapour, carbon dioxide and carbon monoxide main bands as a function of the optical depth and temperature are presented in Table 1.

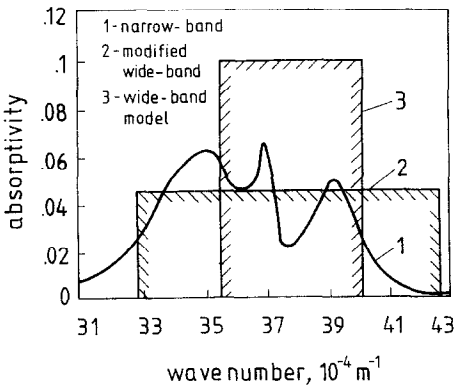

FIG. 1. Spectral absorptivity of 2700 nm band of isothermal H_2O. Path length $L = 0.1$ m, temperature $T = 1500$ K, partial pressure $p_{H_2O} = 10^4$ Pa, total pressure $p = 10^5$ Pa.

3. MODEL TESTING IN A STANDARD NON-HOMOGENEOUS LAYER

The efficiency of the modification will be presented for a non-homogeneous layer characterized by temperature and gas composition distribution assumed by Grosshandler (Fig. 6 in ref. [6]). A numerical procedure was applied in which the total path length was divided into elements of length l. The spectral radiation intensity leaving the Mth element in the path length's direction was calculated by means of equation (1), which in numerical form can be presented as

$$i_M = \exp\left(-\sum_{m=1}^{M} k_\omega l_m\right)\sum_{m=1}^{M} i_{b,m} \times\left[\exp\left(\sum_{m=1}^{M} k_\omega l_m\right)-\exp\left(\sum_{m=1}^{M-1} k_\omega l_m\right)\right]. \quad (3)$$

In the case of the wide-band model, because the band absorptivity is known, equation (3) is replaced by M equations of the same form, the last of which can be written as

$$i_M = i_{M-1}(1-a_M)+a_M i_{b,M}. \quad (4)$$

Results of radiation intensity calculation along the layer depth, divided into nine elements, are presented in Fig. 2 for four models. The modified wide-band model curve almost covers the narrow-band model curve, so that the largest difference does not exceed 3%. The curve obtained for the wide-band model without modification differs from those above. The

Table 1. Main bands absorptivity of the modified wide-band model

Optical depth (Pa m)	Temperature (K) 300	600	1000	1500	2000	2500	Band
Water vapour							
1	0.0045	0.0018	0.00085	0.0005	0.00036	0.00023	
10	0.042	0.016	0.0078	0.0048	0.0033	0.0022	
100	0.25	0.1	0.07	0.04	0.03	0.02	1380 nm
1000	0.5	0.35	0.3	0.27	0.25	0.2	
10 000	0.9	0.7	0.6	0.65	0.8	0.77	
100 000	0.96	0.94	0.92	0.94	0.96	0.96	
1	0.0007	0.0003	0.00015	0.00008	0.00005	0.00004	
10	0.0065	0.0027	0.0014	0.00078	0.00048	0.00038	
100	0.06	0.02	0.013	0.0076	0.0046	0.0036	1870 nm
1000	0.25	0.12	0.1	0.07	0.045	0.036	
10 000	0.6	0.35	0.3	0.35	0.35	0.33	
100 000	0.9	0.67	0.6	0.64	0.65	0.63	
1	0.0005	0.00018	0.00094	0.00005	0.00003	0.00002	
10	0.0047	0.0017	0.009	0.00048	0.0003	0.0002	
100	0.03	0.015	0.085	0.0045	0.003	0.0025	2700 nm
1000	0.16	0.1	0.07	0.042	0.03	0.024	
10 000	0.45	0.3	0.25	0.25	0.22	0.2	
100 000	0.75	0.6	0.55	0.55	0.5	0.45	
1	0.00008	0.000025	0.000013	0.000008	0.000005	0.000004	
10	0.00078	0.00024	0.00013	0.00008	0.00005	0.00004	
100	0.007	0.0023	0.0012	0.00075	0.0006	0.00045	6300 nm
1000	0.05	0.02	0.012	0.008	0.006	0.005	
10 000	0.2	0.08	0.07	0.06	0.055	0.045	
100 000	0.5	0.39	0.35	0.28	0.25	0.2	
1	0.00003	0.00002	0.00001	0.000004	0.0000025	0.0000025	
10	0.0003	0.00019	0.0001	0.00004	0.000025	0.000025	
100	0.003	0.0017	0.001	0.0004	0.0003	0.00025	rotational
1000	0.015	0.01	0.008	0.004	0.003	0.0025	
10 000	0.04	0.03	0.05	0.04	0.03	0.025	
100 000	0.4	0.3	0.5	0.4	0.3	0.25	

Optical depth (Pa m)	Temperature (K) 300	600	1200	1500	1800	2400	Band
Carbon dioxide							
1	0.0025	0.001	0.0004	0.0003	0.0002	0.00014	
10	0.024	0.09	0.0038	0.003	0.002	0.0013	
100	0.2	0.1	0.035	0.03	0.02	0.013	2700 nm
1000	0.8	0.6	0.3	0.3	0.2	0.15	
10 000	0.88	0.9	0.76	0.78	0.75	0.7	
100 000	0.98	0.98	0.98	0.97	0.96	0.95	
1	0.02	0.012	0.005	0.0035	0.0023	0.0013	
10	0.18	0.11	0.045	0.033	0.022	0.013	
100	0.58	0.5	0.3	0.24	0.2	0.13	4300 nm
1000	0.9	0.96	0.96	0.95	0.9	0.7	
10 000	0.97	0.96	0.96	0.96	0.95	0.92	
100 000	0.99	0.98	0.97	0.98	0.97	0.97	
1	0.0004	0.00015	0.000078	0.000067	0.000057	0.00004	
10	0.004	0.0015	0.00075	0.00065	0.00055	0.0004	
100	0.040	0.015	0.008	0.0065	0.005	0.004	15 000 nm
1000	0.25	0.15	0.075	0.06	0.05	0.04	
10 000	0.6	0.6	0.5	0.45	0.45	0.35	
100 000	0.97	0.97	0.96	0.96	0.95	0.93	

Optical depth (Pa m)	Temperature (K) 300	600	1200	1800	2400	Band
Carbon monoxide						
1	0.0012	0.0006	0.0002	0.00012	0.00008	
10	0.0055	0.004	0.0018	0.0011	0.00075	
100	0.018	0.014	0.013	0.009	0.007	4700 nm
1000	0.055	0.045	0.04	0.035	0.033	
10 000	0.13	0.11	0.14	0.125	0.11	
100 000	0.38	0.32	0.35	0.28	0.25	

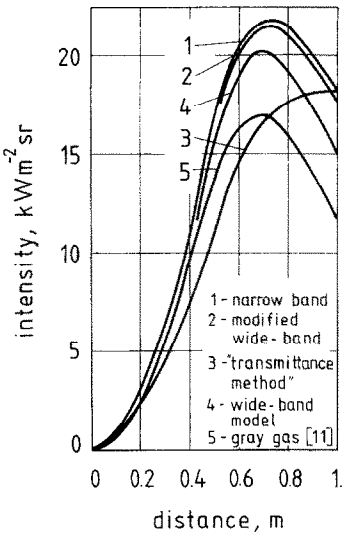

FIG. 2. Comparison of radiation intensity profiles for standard non-homogeneous conditions.

Hottel model of the sum of gray gases with the coefficients of Johnson and Beer [11] gives far worse results due to its limited applicability. It is worth noting that the curve obtained by the 'transmittance method' (equation (13) in ref. [6]) with application of the narrow-band model deforms the intensity curve so that it loses the maximum. This is the outcome of the faulty integral form of the intensity equation (equation (1) in ref. [6]). The TTNH model [6], which gives even worse results than the 'transmittance method', is not presented.

During the testing procedure it was noticed that all the analysed spectral models are sensitive, in certain conditions, to the density of division of the layer depth into elements. Particularly sensitive is the wide-band Edwards model, as a consequence of the too-high value of absorptivity of this model for very small path lengths. This sensitivity was tested for a homogeneous layer divided into elements, because in this case the results ought to be dependent only on the path length of the elements. It has been noticed that the calculated value of radiation intensity for the single homogeneous layer differs from that for the same layer divided into elements. It must be clearly stated here that the reason for this divergence is not the numerical procedure but the nature of the equation describing the spectral properties of the models as a function of the element's path length. The results presented were then obtained for only nine elements because the reference calculations of Grosshandler [6] were done for this number of elements.

4. FLAME TESTING

The suitability of the present modification to prediction of the radiation from a real flame has been tested on a 750 kW natural gas industrial diffusion flame in an experimental combustion chamber, presented in ref. [1]. Because the comprehensive mathematical model of the flame is also influenced by fluid mechanics and chemical kinetics data, to avoid a wrong interpretation of results it was decided that, in the verification procedure, the experimental values of temperature, gaseous chemical composition and soot concentration would be used. The linear spectral coefficient of soot absorption was calculated based on Mie theory from the equation [9]

$$k_{\nu} = 36\pi cnk/[(n^2-k^2+2)^2+4n^2k^2]\rho \qquad (5)$$

where values of n and k were obtained from ref. [16]. The scattering of radiation on soot particles was neglected, because measurements show that diameters of soot in flame are smaller than 80 nm.

The intensity of flame radiation in a direction perpendicular to the flame axis was measured by a narrow-angle probe equipped with a total radiation pyrometer. During the measurements a cold black body was placed at the background of the flame. The concentration of soot was obtained by a sampling probe in which combustion products were diluted by nitrogen. Figures 3 and 4 present measured traversal distributions of the flame parameters at two distances along the axis. Calculations were based on equation (4), with application of 38 elements along the path length, because the traversal experimental data were obtained at this number of points. Results are presented in Fig. 5 for a distance along the flame axis 0.6 m from the burner mouth, together with the experimental data of radiation intensity. The narrow-band model and the modified wide-band model describe the measured results reasonably well.

The model has also been tested on the sensitivity of the number of elements. Calculations were made for 13 and 26 elements. Radiation intensity at the end of the path length for the three analysed models is

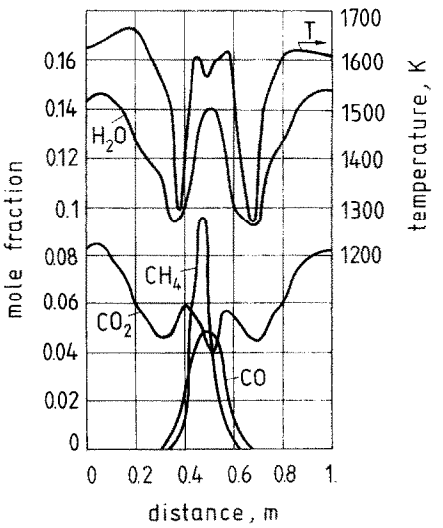

FIG. 3. Composition and temperature profiles measured within the natural gas flame. Distance from burner exit 0.6 m. Chamber pressure 10^5 Pa.

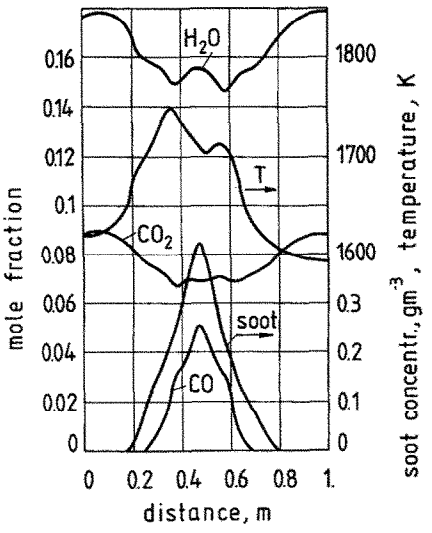

FIG. 4. Composition, soot concentration and temperature profiles measured within the natural gas flame. Distance from burner exit 1.3 m. Chamber pressure 10^5 Pa.

presented in Table 2. It can be seen that, for the conditions of analysis, the narrow-band model is almost insensitive to the number of elements. The most sensitive is the Edwards wide-band model. Assuming the results of the narrow-band model as standard values we can say that, for division of the flame into 38 elements, the Edwards wide-band model gives results with an error of 27%, while the modified wide-band model reduced this error to only 7%.

During the calculations the radiation properties of methane were taken from Edwards' wide-band model, without modification, because insufficient information of the narrow-band model data for methane did not allow the model modification for this component of the flame. We believe that if such modification were made it would further improve the accuracy of modelling.

The calculated results of radiation intensity for a

Table 2. Calculated radiation intensity for various numbers of elements; distance from burner exit 0.6 m

Number of elements	Radiation intensity (kW m^{-2} sr^{-1})		
	Wide-band model	Modified wide-band model	Narrow-band model
13	23.69	27.24	27.87
26	22.39	27.63	27.60
38	19.77	25.53	27.30

1.3 m distance from the burner mouth along the flame axis are presented in Fig. 6. The differences between the values of intensity obtained by the analysed gas radiation models are smaller than those presented in Fig. 5. This is due to the high soot concentration at 1.3 m, giving intense luminous radiation which covers the differences between the gas radiation models.

5. CONCLUSION

The presented modification of the wide-band model allows application to non-homogeneous layers with satisfying accuracy.

The narrow-band model and the modified wide-band model stabilize with an increasing number of elements, while the Edwards wide-band model gives increasing error.

The still-existing differences of results with the narrow-band model and with the modified wide-band model are due to the approximations of the equivalent gas wide-band area given by Edwards. This error, however, is smaller than 10% in extreme cases.

Dividing the range of the wave number into the same elements, the time of calculation by the wide-band model is about eight times shorter than by the narrow-band model.

Radiation intensity from large diffusion flames can

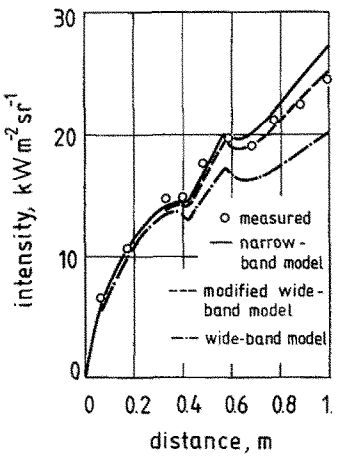

FIG. 5. Comparison of the calculated and measured radiation intensity values for a natural gas flame. Distance from burner exit 0.6 m.

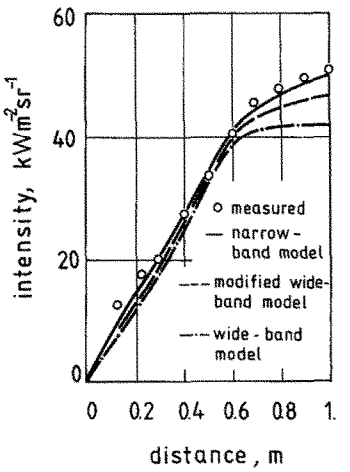

FIG. 6. Comparison of the calculated and measured radiation intensity values for a natural gas flame. Distance from burner exit 1.3 m.

be predicted satisfactorily by the modified wide-band model with absorptivities presented in Table 1.

REFERENCES

1. Z. Gebhardt and J. Tomeczek, The emissivity of natural gas diffusion flames, *Gas Wärme Int.* No. 11, 329–334 (1982).
2. R. M. Goody, *Atmospherical Radiation. I. Theoretical Basis*. Clarendon Press, Oxford (1964).
3. D. K. Edwards and W. A. Menard, Comparison of methods for correlation of the total band absorption, *Appl. Optics* **3**, 621–625 (1964).
4. D. K. Edwards, Molecular gas band radiation. In *Advances in Heat Transfer* (Edited by T. F. Irvine, Jr. and J. P. Hartnett), Vol. 12, pp. 115–193. Academic Press, New York (1976).
5. H. C. Hottel and A. F. Sarofim, *Radiative Transfer*. McGraw-Hill, New York (1967).
6. W. L. Grosshandler, Radiative heat transfer in non-homogeneous gases: a simplified approach, *Int. J. Heat Mass Transfer* **23**, 1447–1459 (1980).
7. R. D. Cess and L. S. Wang, A band absorptance formulation for non-isothermal gaseous radiation, *Int. J. Heat Mass Transfer* **13**, 547–555 (1970).
8. S. H. Chan and C. L. Tien, Infrared radiative heat transfer in non-isothermal gases, *Int. J. Heat Mass Transfer* **14**, 19–26 (1971).
9. R. Viskanta and M. P. Menguc, Radiation heat transfer in combustion systems, *Prog. Energy Combust. Sci.* **13**, 97–160 (1987).
10. P. B. Taylor and P. J. Foster, The total emissivities of luminous and non-luminous flames, *Int. J. Heat Mass Transfer* **17**, 1591–1604 (1974).
11. T. R. Johnson and J. M. Beer, The zone method analysis of radiant heat transfer, a model for luminous radiation, *J. Inst. Fuel* **46**, 301–309 (1973).
12. V. Emmerich, Der Einfluss des Flammenruss auf die Strahlungswarmeubertragung in Flammen und Feuerramen, Ph.D. Dissertation, Universitat Fridericiana, Karlsruhe (1985).
13. B. Leckner, Some elements of radiative heat transfer calculation in flames and gases, *Archiwum Prosesow Spalania* **4**, 377–398 (1973).
14. R. Siegel and J. R. Howell, *Thermal Radiation Heat Transfer*, (eq.XIV-10), 2nd edn. McGraw-Hill, New York (1981).
15. C. B. Ludwig, W. Malkmus, J. E. Reardon and J. A. Thomson, *Handbook of Infrared Radiation from Combustion Gases*, NASA SP-3080 (1973).
16. S. C. Lee and C. L. Tien, Optical constants of soot in hydrocarbon flames, *Eighteenth Symp. (Int.) on Combustion*, pp. 1156–1166 (1981).

MODIFICATION DU MODELE DE RAYONNEMENT DE GAZ A LARGE BANDE POUR LE CALCUL DE FLAMME

Résumé—On présente une modification du modèle de gaz à large bande convenable pour une couche non homogène. L'application de cette modification est comparée avec les modèles déjà connus du rayonnement dans la condition standard et dans une flamme à forte diffusion. On montre que la modification conduit à l'accroissement de la précision du calcul de l'intensité du rayonnement par le modèle à large bande. Une vérification expérimentale est présentée pour une flamme de gaz naturelle de 750 kW.

MODIFIKATION DES MODELLS FÜR DIE BREITBAND-GASSTRAHLUNG BEI DER BERECHNUNG VON FLAMMEN

Zusammenfassung—In der vorliegenden Arbeit wird eine Modifikation des Modells für Breitband-Gasstrahlung vorgestellt, die für inhomogene Schichten geeignet ist. Die Anwendung dieser Modifikation wurde mit Modellen für Strahlung unter Standardbedingungen in der Literatur und mit großen Diffusionsflammen verglichen. Es wird gezeigt, daß die vorgeschlagene Modifikation eine genauere Berechnung der Strahlungsintensität mit dem Breitbandmodell erlaubt. Die berechnete Strahlungsintensität für eine Gasflamme mit einer Leistung von 750 kW wird experimentell bestätigt.

МОДИФИКАЦИЯ ШИРОКОЗОННОЙ МОДЕЛИ ИЗЛУЧЕНИЯ ГАЗА ДЛЯ РАСЧЕТА ФАКЕЛА

Аннотация—Целью настоящего исследования является модификация широкозонной модели излучения газа для случая неоднородного слоя. Результаты использования модифицированной модели сравниваются с имеющимися в литературе данными для моделей излучения в нормальных условиях и при больших диффузионных пламенах. Показано, что предложенная модификация позволяет повысить точность расчета интенсивности изучения с помощью широкозонной модели. Приводится экспериментальное подтверждение расчетных результатов по интенсивности изучения для естественного газового факела мощностью 750 кВт.